Novel imaging system for measuring microscale curvatures at high temperatures

Haruna Tada, Amy E. Kumpel, Richard E. Lathrop, and John B. Slanina
Thermal Analysis of Materials Processing Laboratory, Tufts University, Medford, Massachusetts 02155

Patricia Nieva and Paul Zavracky
Microfabrication Laboratory, Northeastern University, Boston, Massachusetts 02115

Ioannis N. Miaoulis and Peter Y. Wong[a)]
Thermal Analysis of Materials Processing Laboratory, Tufts University, Medford, Massachusetts 02155

(Received 13 August 1999; accepted for publication 6 October 1999)

An innovative system was designed to optically measure the curvature of microelectromechanical system at high temperatures. The system takes advantage of the limited numerical aperture of the imaging system to detect the curvature of cantilever beams. Images of the beam are used to determine beam curvature at high temperatures of up to 850 °C by analyzing the apparent change in beam length as seen by the camera during an experimental trial. The system is designed to operate at very high temperatures, which is difficult in conventional microscale curvature measurement techniques such as scanning electron microscopy or stylus profilometry due to excess heating of peripheral equipment. The system can measure curvatures as small as 300 m^{-1}, which corresponds to tip deflections of 1.5 μm for a 100 μm beam. The resolution of the system is limited by the image resolution of the charge-coupled device camera, and increases at large curvatures. The maximum curvature that can be measured by the system is limited by the increase in system resolution, and is estimated to be 4500 m^{-1}, corresponding to 22 μm deflection for a 100 μm beam. The apparatus was demonstrated to measure the thermally induced curvature of multilayered thin-film cantilever beams. The beams bend at high temperatures due to mismatch in thermal expansion coefficients between the layers. One innovative application of such curvature measurement is the determination of thermophysical properties of thin films at elevated temperatures. This article presents the experimental setup and operational theory of apparatus, as well as curvature measurements obtained by the system. The thermal expansion coefficient of polycrystalline silicon, determined from the curvature measurements, are also discussed. © *2000 American Institute of Physics.*
[S0034-6748(00)04401-4]

I. INTRODUCTION

Application of silicon-based thin-film materials, which were conventionally used as electrical components in integrated circuits, are extending to mechanical components due to development of microelectromechanical systems (MEMS) technology. As this transition is made, the need for determination of thermophysical properties of thin films is growing. Properties of interest include Young's modulus, deposition or residual stress, thermal expansion coefficient, and Poisson's ratio. Furthermore, as MEMS applications extend to high temperatures, properties at temperatures exceeding 800 °C are desired to address all practical temperature range.

Curvatures of multilayered structures, induced by the differences in the mechanical properties and stress states of the layers, can yield valuable information about the properties that caused the curvature. A technique was developed to determine the thermal expansion coefficients (α) and Young's moduli (E) of thin film layers as functions of temperature, based on the thermally induced curvature of multilayered cantilever beams.[1] Techniques for determining Young's modulus have been developed for room temperature, including deflection of cantilevers,[2,3] measurement of the resonance frequencies of micromachined structures,[4–7] bulge testing of membranes,[8,9] and direct tensile testing of thin film specimen.[10–12] However, these methods generally cannot be applied to high temperatures due to delicate instrumentation used. Study of thermal expansion coefficients of thin films have been more challenging; experimentation at high temperature is a necessity for the determination of α, leading to difficulties in experimental design and implementation. Measurement of thermally induced curvature is a unique technique which allows the determination of material properties at high temperatures.

Measurement of stress-induced curvature on the wafer level has been demonstrated for the determination of residual stresses in thin film layers.[13] In these cases, the curvature is measured optically using lasers, or by interferometry, or mechanically by stylus profilometers.[14] However, because residual stress is a combination of deposition and thermal stress, thermally induced curvature is generally smaller in magnitude than curvatures due to residual stress. Thermally induced curvature of wafer due to thin film is typically very

a)Author to whom correspondence should be addressed; electronic mail: pwong@tufts.edu

small due to the relatively large thickness of the wafer, and cannot be readily measured. In order to induce large curvatures, multilayered thin film cantilever beams were designed.[15]

Optical curvature measurement techniques that are used on the wafer-level cannot be adapted to microscale curvature measurements. Curvatures of micromachined thin film structures are typically measured by a stylus profilometer or from a scanning electron microscopy (SEM) micrograph.[16] Both of these instruments cannot be applied at extremely high temperatures due to excessive heating of peripheral equipment that are often in close proximity to the sample. Furthermore, SEM requires a clear side-view of the beams in order to determine curvature, and therefore is difficult to measure negative curvature as the beams bend into the Si substrate. Optical techniques for measuring curvatures of microstructures, such as laser profilometry, also have limited operating temperatures. In order to measure curvatures of micromachined structures at high temperatures, an innovative experimental technique was developed.

The apparatus is a novel system designed to optically measure curvature of the beams at temperatures as high as 850 °C. The optical system consists of three primary components. A fiber-optic light source illuminates the sample from above with collimated light, a charge-coupled device (CCD) camera is used to visualize the beams for curvature analysis, and a tungsten-halogen lamp heats the sample from below to temperatures as high as 850 °C. During heating and cooling, temperature near the sample is recorded by a thermocouple while the CCD camera takes images of the beams. Due to the limited numerical aperture of the camera, only the nearly flat portion of the sample is seen by the camera. This results in an apparent change in beam length on the image as the curvature changes. Each image taken during an experiment is postprocessed to determine the apparent beam length as seen by the CCD camera at any given temperature. The curvature is found by relating the geometry of the curved beam and its apparent length.

The structures used for the material property determination consist of multilayered cantilever beams (polycrystalline silicon and silicon dioxide) suspended over a silicon substrate by a 25 μm gap. A SEM micrograph of the beams is shown in Fig. 1. The beams are between 100 and 50 μm long, and consist of (from top): 0.19 μm SiO_2, 0.54 μm poly-Si, and 1.03 μm SiO_2. As seen in Fig. 1, these structures typically have an upward curvature at room temperature due to residual stress from fabrication. Because the thermal expansion coefficient of SiO_2 is less than that of poly-Si, the beams bend down at high temperature. Thermophysical properties of the thin film materials can be found at high temperatures by measuring the thermally induced curvature and applying a numerical model developed by Townsend and Barnett,[17] which relates the curvature of a multilayered beam to its geometry and thermophysical properties.

In addition to application for determining $E(T)$ and $\alpha(T)$, curvature of cantilever beams are often used to determine residual stress gradients in thin films.[16,18] Because this system is designed for operation at very high temperature, possible future applications include the study of stress relaxation or annealing effects in thin films using cantilever beams. Generally, such studies are done through an *ex situ* measurement of curvature after the sample has cooled to room temperature. *In situ* measurement of beam curvature at high temperatures would provide more accurate understanding of effects of high temperature on thin film stresses.

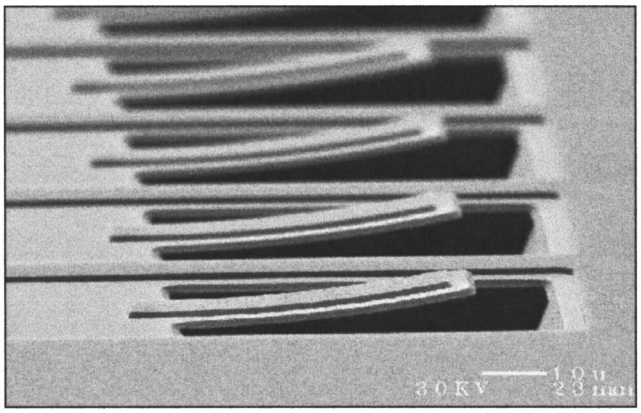

FIG. 1. SEM micrograph of multilayered cantilever beam. The beams shown are approximately 50 μm long, and consist of poly-Si top layer and SiO_2 bottom layer. The beams are suspended over Si substrate by a 25 μm gap.

This article presents the design of the experimental system, as well as the theory of its curvature measurement. Limitations of the system are also discussed. Experimental results for the measurement of thermally induced curvature of multilayered beams are also presented.

II. EXPERIMENTAL SETUP

Figure 2 shows the schematic of the experimental setup. The sample holder is shown in plan-view in Fig. 2(b). The die containing the sample is cut to $\sim 4\,\text{mm} \times 4\,\text{mm}$, and is supported by a 4 in. Si wafer resting on two parallel quartz rods. The silicon wafer that supports the wafer also serves to block the visible light from the heater in order to maintain constant image brightness during heating. The quartz rods must be supported in such way that it does not deflect by the weight of the Si wafer. Furthermore, it must be able to slide freely in axial direction in order to prevent deflection from thermal strain at high temperatures.

The sample is illuminated from above by collimated light source. The light source consists of a fiber optic bundle with an achromatic lens for collimation. Achieving good collimation is critical in the operation of the system, as will be discussed in a later section. A cube beamsplitter is used to direct the light to normal incidence. Cube or pellicle beamsplitter is necessary in this application; ghost images resulting from multiple reflections in a conventional beamsplitter result in a poor image quality that cannot be used to determine curvature. A CCD camera equipped with a telescopic lens is used for visualization of the sample. The lens system has a minimum field-of-view of approximately 400 μm. The pixel-to-length conversion for the optical system was found using an image of a reticle; this conversion factor is used during image analysis.

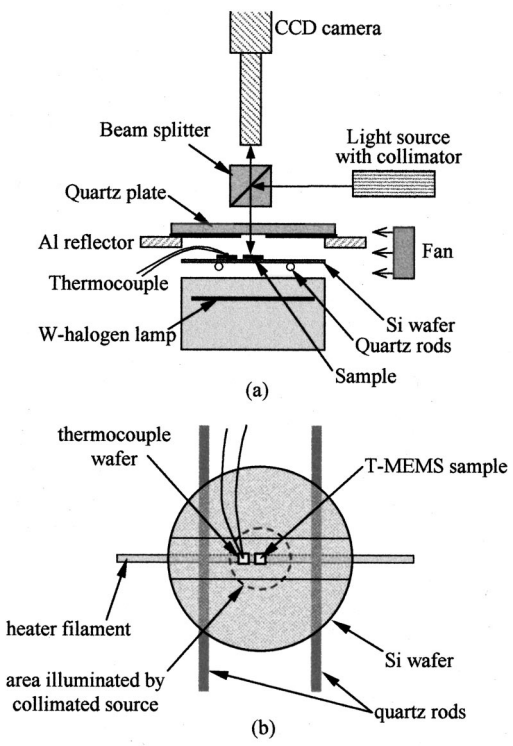

FIG. 2. Schematic of the experimental setup. (a) Side-view, and (b) plan-view of the sample holder. The sample is heated from below by W-halogen lamp and is illuminated from above by collimated light source. Images of beam are captured by a CCD camera for image processing.

The sample is heated from below by a tungsten-halogen lamp to temperatures exceeding 850 °C. The heater has a parabolic reflector in the housing, which concentrates the radiation into a line. The nonuniform heating from the lamp results in a large thermal gradient in the Si support wafer. To prevent wafer deformation, and thus change in position of the sample, during heating, the wafer was cut into three pieces, the center one being ~2 cm wide. All three pieces must still be used in order to shield the visible light from the CCD camera. Temperature during heating is monitored by a type-*R* thermocouple embedded in a small Si wafer (Sensarray), which is cut to resemble the sample die. The thermocouple die lies near the sample during heating in order to accurately represent the temperature reached by the sample.

The thermally induced curvature of a beam is calculated from the apparent change in the beam length as received by the CCD camera. Because data analysis is directly associated with image quality, any distortion or change in image during an experiment affects the accuracy of the data. Specifically of concern are image distortion due to natural convection currents at high temperature and change in image brightness due to visible light emitted by the heater. Peripheral components were incorporated into the experimental design to minimize these effects.

Image distortion from natural convection current is due to the temperature-dependent index of refraction of air. Natural convection sends pockets of warm air rising into cooler air, which cause light to refract as index of refraction changes. The effect can be reduced by minimizing the current, and by enhancing the mixing of warm and cool air to reduce the temperature gradient which causes refraction. Natural convection current is reduced considerably by limiting the vertical space above the sample, and this is accomplished by placing a quartz plate approximately 5 cm above the sample. The small space greatly limits the amount of natural convection directly above the sample. The quartz plate is supported by an aluminum plate with a 10 cm window in the center. The quartz plate is covered with aluminum foil, with the exception of a 4-cm-diam window in the center for visualization of the sample. The aluminum plate and foil enhances heating by reflecting radiation from lamp and the heated sample back onto the wafer. In addition, they help keep the camera and other system components cool by preventing radiation from reaching them. To further improve image quality, a fan is mounted in the system with airflow directed to pass over the sample, both below and above the quartz plate. Forced air from the fan eliminates temperature gradients in the convection currents passing over the sample.

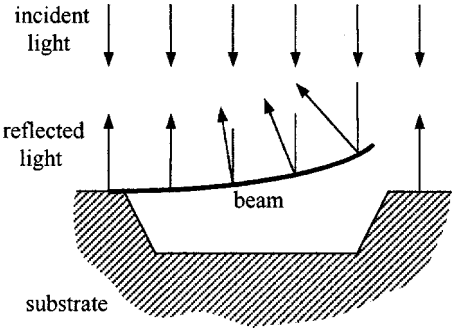

FIG. 3. Reflection of normally incident, collimated light from a curved beam. Due to the curvature of the beam, rays near the tip of the beam are reflected at a greater angle than the rays near the base of the beam. This results in an apparent length of the beam, which is generally smaller than the actual beam length.

Any visible light from the heater that is captured by the CCD camera introduces error in the data by changing the brightness of the image during an experiment. To eliminate this error, it is crucial that the three pieces of Si wafer are aligned with no spaces between the individual pieces. The aluminum plate, mentioned above, also contributes to reducing this error. The window in the aluminum plate may be no larger than the diameter of the Si support wafer; this further ensures that no visible light from the filament leaks into the camera during heating.

III. THEORY

Figure 3 illustrates the reflection of collimated light from a curved cantilever beam. The beam is curved in such way that it forms an arc of a complete circle with radius *R*. This assumption implies that the curvature, *K*, along the length of the beam is constant. The light reflects by obeying the law of reflection locally; therefore, at each point on the beam, the incident angle is equal to the angle of reflection. Consequently, the incident light near the tip of the beam reflect at a greater angle from vertical than the light that strikes at the base. Because the numerical aperture of the optical system is limited, only the rays reflecting at a small angle from the

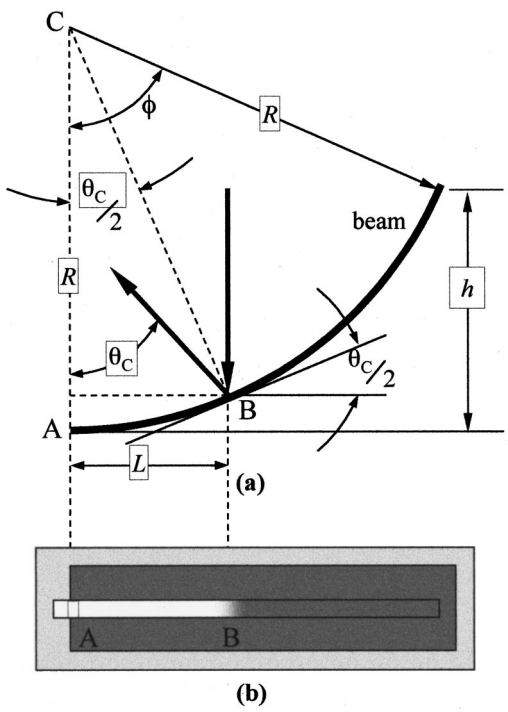

FIG. 4. Geometry of beam for normally incident light; (a) side-view, and (b) top-view seen by the CCD camera. For an optical system with cone angle of θ_c, a beam having radius of curvature R appears to have an apparent length of L. In such case, the angle between the beam and horizontal at L is equal to $\theta_c/2$.

vertical is detected by the CCD camera. The result of this effect is an apparent length of the beam, L, that is seen by the camera.

Figure 4 illustrates the geometrical relation between incident light and the beam. For a beam having an apparent beam length equal to the distance AB, incident light at point B reflects at an angle θ_c from the vertical. This angle defines the ''cone angle'' of the system, which is a measure of the numerical aperture of the optical system. The angle θ_c is the largest angle at which light can be detected by the camera, and is a constant in the experimental setup, regardless of the curvature of the beam. By geometry, the angle from the vertical to the normal of the beam at point B is $\theta_c/2$. Recall that the beam is assumed to be an arc of a circle with radius R. By geometry, the angle between the system horizontal and the beam at point B is also $\theta_c/2$.

The geometrical relation between θ_c and the beam curvature, K, is given by

$$L = R \sin\frac{\theta_c}{2} \Rightarrow \quad K = \frac{1}{R} = \frac{\sin(\theta_c/2)}{L}, \tag{1}$$

where L is the apparent length of the beam. Based on this equation, curvature can be found for any beam by characterizing θ_c, which is the property of the optical system, and L, the apparent length of the beam.

The beam forms an arc angle, ϕ, of a complete circle, given by

$$\phi = \frac{L_{\text{arc}}}{R}. \tag{2}$$

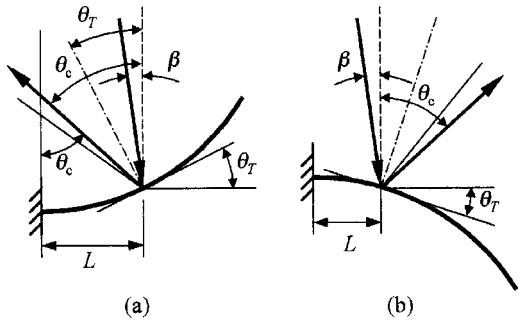

FIG. 5. Geometry of beam for a misaligned system for (a) positive curvature, and (b) negative curvature. The angle between beam and horizontal at L is equal to θ_T, which may be smaller or larger than $\theta_c/2$.

The geometric relation between the beam tip deflection, h, and R can be described using ϕ:

$$h = R(1 - \cos\phi). \tag{3}$$

Combining Eqs. (2) and (3) results in the following relation:

$$h = R\left(1 - \cos\frac{L_{\text{arc}}}{R}\right). \tag{4}$$

The significance of this equation is that it relates the radius of curvature to two, readily available quantities. At room temperature, h can be measured using an ordinary optical microscope to an accuracy of ± 0.5 μm. The arc length is equal to the total length of the beam, which can also be measured by a microscope. From the two quantities, the radius of curvature of a beam at room temperature can be solved iteratively from Eq. (4).

Rearranging Eq. (1) results in the following expression for θ_c:

$$\theta_c = 2 \sin^{-1}\frac{L}{R}. \tag{5}$$

An analysis of room temperature image taken by the CCD camera results in the apparent beam length, L. Since the radius of curvature at room temperature was found above, the cone angle of the system can be found from Eq. (5). Recall that the cone angle is a constant for an experimental trial, independent of beam curvature and temperature. Therefore, using the θ_c found at room temperature, all beam curvatures in the trial are determined from Eq. (1) by applying image analysis to beam images at different temperatures to find L.

The geometric relations found above assume that the light, sample, and camera are perpendicular with respect to each other. However, due to imperfections in the system alignment, there is a small misalignment angle, β, between the components. This is illustrated for positive and negative curvatures in Fig. 5. The effect of β is nonsymmetrical about the zero curvature, and must be considered separately for positive and negative curvatures. Note that the misalignment shown in Fig. 5 is greatly exaggerated; in practice, β is typically less than 0.1°.

To correct for the misalignment angle, the angle between the beam and horizontal (previously equal to θ_c) is redefined as θ_T. Again, θ_c is the cone angle of the system, a constant

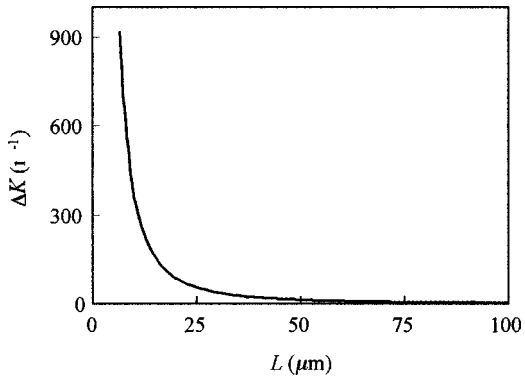

FIG. 6. Curvature resolution of the system, shown as a function of apparent beam length. The resolution increases rapidly at small beam lengths (large curvatures). This increase in resolution defines the upper limit of the curvature range of the system.

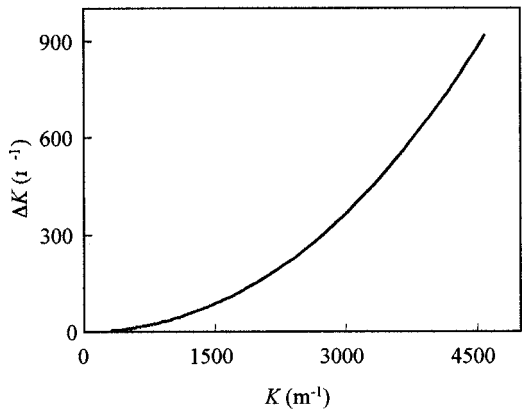

FIG. 7. Curvature resolution of the system, shown as a function of curvature. The resolution increases for increasing curvatures, limiting the curvature range that can be measured by the system.

through an experiment. Due to the misalignment, the angle between the beam and horizontal is no longer equal to θ_c, and is geometrically determined to be

$$\theta_T = \frac{\theta_c + \beta}{2}. \tag{6}$$

For negative beam curvatures, the angles are related by

$$\theta_T = \frac{\theta_c - \beta}{2}. \tag{7}$$

In a misaligned system, Eq. (5) becomes

$$\theta_T = 2 \sin^{-1} \frac{L}{R} \tag{8}$$

and this expression is used to determine θ_T at room temperature. For a beam that is initially bending up, which is typically the case, Eq. (6) is then applied to find θ_c, which is a constant for the system. For all subsequent images, curvatures are found from Eq. (8) by using the expression for θ_c for the curvature direction. Notice that the effect of β on the curvature data depends upon the direction of the initial beam curvature. If the beam has a positive initial curvature, then results for positive curvatures is unaffected by the angle β. However, results with negative curvature must be corrected to account for the change in sign between Eqs. (6) and (7).

The curvature resolution (ΔK) of system, defined as the smallest change in curvature that the system can detect, is determined by the spatial resolution of the CCD camera. The resolution corresponds to the change in curvature that results from a change in the apparent beam length of one pixel. Due to the nonlinear relation between L and K, the resolution varies nonlinearly with L as shown in Fig. 6. The corresponding ΔK as a function of curvature is shown in Fig. 7. The system resolution improves with decreasing curvature values as shown in Fig. 7. The system resolution shown in the figure is calculated for a θ_c of 0.06 radians, which is typical of the optical system used in this setup.

The theoretical limit for the maximum curvature measured by the optical system corresponds to the curvature of the beam at an apparent length of one pixel. However, as shown in Fig. 6, the resolution of the system increases rapidly at small apparent beam lengths. To approximate the practical maximum detection limit of the system, an upper limit for ΔK was defined to be 20% of the corresponding curvature value. The maximum curvature limit based on the new criteria was found to be approximately 4500 m^{-1}, with a resolution of 900 m^{-1}. This value corresponds to an apparent beam length of approximately 6.5 μm and a tip deflection of 22 μm for a 100 μm beam.

The minimum curvature measured by the system corresponds to the curvature at which the beam tip is at an angle $\theta_c/2$ with the horizontal. Beams having curvatures smaller than this value will appear to have an apparent length equal to the actual length of the beam. For a 100 μm beam, measured at θ_c of 0.06 radians, the minimum curvature that can be detected is approximately 300 m^{-1}, corresponding to a beam tip deflection of 1.5 μm. Curvature for beams having an apparent length equal to the actual length are assigned to a value of zero curvature during data analysis.

IV. EXPERIMENTAL PROCEDURE

A typical optical microscope at $\times$500 magnification is used to measure beam tip deflection at room temperature. The vertical translation of the microscope is calibrated at 1 μm resolution, and the uncertainty of the measurement is estimated at $\pm$ 0.5 μm. Tip deflection at room temperature typically ranges between 7 and 10 μm, upward. This value is used to calculate θ_c of the system at room temperature. After measuring the tip deflection, the sample is positioned on the center of the supporting silicon wafer as shown in Fig. 2(b). Figure 8 shows an image of the sample as seen by the CCD camera, centered in the field of view with the base of the beam on the left. The beams in Fig. 8 have an upward deflection of approximately 7 μm, and therefore a correspondingly small apparent length. Because images are used directly for the determination of curvature, it is necessary for the image to have a consistent focus throughout the experiment. During heating, the change in temperature of the quartz plate, as well as of the air between sample and camera, results in a variation in the index of refraction. The change affects the focusing of the camera, particularly at very high temperatures. In order to minimize error due to inadequate focusing, the image must be refocused through-

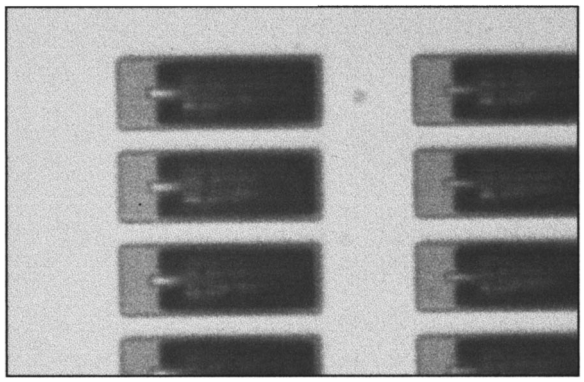

FIG. 8. Image of beams as seen by the CCD camera. The beams shown have an upward curvature of approximately 7 μm, resulting in a small apparent beam length, L.

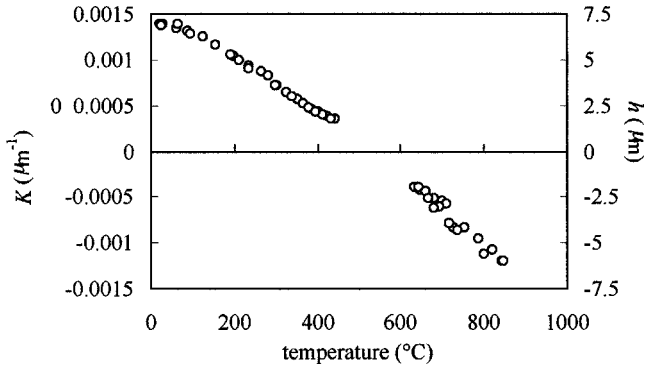

FIG. 10. Beam curvature and tip deflection at high temperatures for a 100 μm beam. The data shown are for one heating-cooling cycle. The absence of data near zero curvature indicates the region where the beam curvature was less than system range.

out the trial. If not properly focused, an error of up to 2% may be introduced into the curvature calculations.

An image is taken at room temperature to establish the initial experimental conditions, used to calculate θ_c. During heating, the temperature indicated by the thermocouple die is recorded by a LabVIEW program. The sample reaches a maximum temperature of ~850 °C. Note that the maximum temperature is a consequence of the limit of the heat source; the system can be used at even higher temperatures if a stronger heat source were used. After the sample has reached the maximum temperature, the heat is turned down to allow the sample to cool down to room temperature. Throughout the experimental trial, which typically consists of both the heating and cooling phases, grayscale images of the beams are taken at regular intervals. The final picture is taken once the sample has cooled to room temperature.

In order to determine the apparent beam length of each image, the grayscale values along a row in the image are obtained through image processing software. Figure 9 shows the grayscale along a row on a representative beam. A ''grayscale threshold value'' is entered by the user, defining

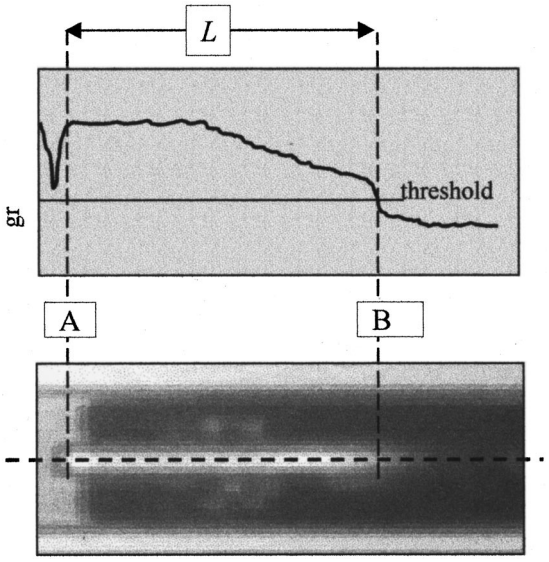

FIG. 9. Grayscale analysis of an image. The apparent beam length, L, is determined by comparing the threshold value to the grayscale values along the beam, shown by the dotted line on the image.

the apparent length of the beam as seen on the CCD camera. The number of pixels from point A to point B of Fig. 9 is equal to the apparent beam length L, scaled by the pixel-to-millimeter resolution of the camera. The apparent length at each temperature is used to calculate $K(T)$ from Eq. (1). Notice that the apparent beam length for any given image is a function of the threshold value selected by the user. In fact, the value used for the threshold value may change L up to 10 μm. This variation does not introduce significant error to the curvature measurement since all images are processed using the same threshold and thus are affected by the same change. The user may therefore select any value that lies between the bright and dark portions of the beam as the threshold; however, it should be noted that a higher threshold value (closer to the bright portion) will result in a smaller L and θ_c, leading to a smaller minimum curvature limit of the system.

V. RESULTS

A graph of the beam curvature and deflection during one heating and cooling cycle is shown in Fig. 10. In the case shown, the 100 μm beam has an initial tip deflection of 7 μm. At the maximum temperature, the beam deflection is approximately -7 μm. The beam returns to its original position upon cooling to room temperature. The points on the diagram which have curvature values of zero are those points which fall below the minimum curvature limit of the system. The lack of data in this region can be accounted for by analyzing a set of beams with different initial deflections but having the same film structure. Beams having different initial deflections will pass through zero curvature at different temperatures, and compilation of data from a set of such beams will yield a full range of $K(T)$ data. The initial curvature of the beams was found to decrease with long exposure to temperatures above 800 °C; therefore, high temperature annealing process can be used to generate beams with different initial deflection.

Curvature measurements shown in Fig. 10 was used to determine the thermal expansion of poly-Si thin films at temperatures up to 300 °C.[19] Thermally induced curvature of multilayered beams is a function of thermal expansion coefficient and Young's moduli of the layers, and can be found numerically be method developed by Townsend and

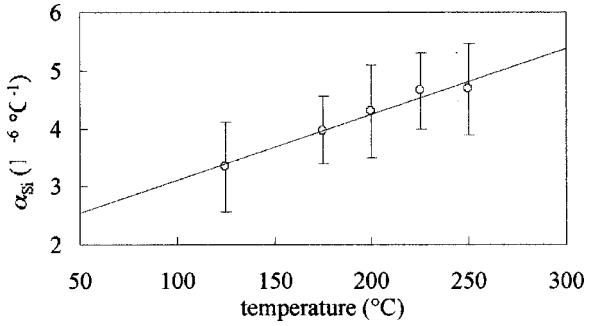

FIG. 11. Thermal expansion coefficient of poly-Si thin films (Ref. 19). Values shown were determined based on curvature measurements in Fig. 10. Vertical bars indicate the standard deviation over seven sets of curvature data. E_{Si}, E_{SiO_2}, and α_{Si} were approximated using published values.

Barnett.[17] The property α_{Si} was determined by approximating E_{Si}, E_{SiO_2}, and α_{SiO_2} by published values. The layer thickness of the beam used are such that the curvature is minimally affected by E; therefore, using approximate values for E introduces negligible error in the analysis. Temperature-dependent values of E_{Si} were used as reported by Kahn *et al.*[7] Young's modulus of SiO_2 was assumed to be a constant for temperatures up to 300 °C, and a value of 64 GPa was used.[20] For temperatures below 300 °C, thermal expansion coefficient of silica glass materials are generally constant, and published value of $5\times10^{-7}\,°C^{-1}$ was used through the temperature range.[21] A linear variation in $\alpha_{Si}(T)$ was assumed for temperatures between 50 and 300 °C. Figure 11 shows the α_{Si} found from application of curvature measurements in five temperature intervals. The vertical bars at each location indicate the standard deviation over seven sets of data. The $\alpha_{Si}(T)$ values found using five intervals of curvature measurements closely follow a linear trend. The results indicate that α of poly-Si thin films are higher than α for bulk, crystalline Si. The numerical technique used to determine α_{Si}, as well as results for higher temperature range, is discussed in more detail in Ref. 19.

Curvature data can also be used for characterizing other mechanical properties of thin films at high temperatures, such as Young's modulus, by modifying the design of multilayer thickness.[1] Thin film properties are of great interest to the growing MEMS industry, where thin films are used as mechanical components in microscale devices. Alternatively, curvature of thin films are often used to determine residual stresses in thin film layers. Measurement of beam curvatures at high temperatures allows the *in situ* analysis of stress relaxation during annealing at high temperatures.

ACKNOWLEDGMENTS

The authors gratefully acknowledge the support of this research by the National Science Foundation under Grant Nos. DMI-9612068 and EEC-9732073.

[1] H. Tada, A. E. Kumpel, R. E. Lathrop, J. B. Slanina, Patricia Nieva, Paul Zavracky, I. N. Miaoulis, and P. Y. Wong (unpublished).
[2] Johansson and J-Å. Schweitz, J. Appl. Phys. **63**, 4799 (1988).
[3] P. T. Jones, G. C. Johnson, and R. T. Howe, Mater. Res. Soc. Symp. Proc. **518**, 197 (1998).
[4] H. Kahn, S. Stemmer, R. L. Mullen, M. A. Huff, and A. H. Heuer, Mater. Res. Soc. Symp. Proc. **403**, 321 (1996).
[5] H. Kahn, S. Stemmer, K. Nandakumar, A. H. Heuer, R. L. Mullen, R. Ballarini, and M. A. Huff, Proceedings of IEEE International Workshop on Microelectromechanical Systems, 1996 (unpublished), p. 343.
[6] S. Lee, C. Cho, J. Kim, S. Park, S. Yi, J. Kim, and D. Dan Cho, Mater. Res. Soc. Symp. Proc. **518**, 21 (1998).
[7] H. Kahn, M. A. Huff, and A. H. Heuer, Mater. Res. Soc. Symp. Proc. **518**, 33 (1998).
[8] S. Jayaraman, R. L. Edwards, and K. J. Hemker, J. Mater. Res. **14**, 688 (1999).
[9] O. Tabata, K. Kawahata, S. Sugiyama, and I. Igarashi, Proceedings of the IEEE Workshop on Microelectromechanical Systems, 1989 (unpublished), p. 152.
[10] W. N. Sharpe, Jr., K. Turner, and R. L. Edwards, Mater. Res. Soc. Symp. Proc. **518**, 191 (1998).
[11] S. Greek and F. Ericson, Mater. Res. Soc. Symp. Proc. **518**, 51 (1998).
[12] W. N. Sharpe, Jr., B. Yuan, and R. L. Edwards, J. Microelectromech. Syst. **6**, 193 (1997).
[13] J. Y. Robic, H. Leplan, M. Berger, P. Chaton, E. Quesnel, O. Lartique, C. Pelle, Y. Pauleau, and F. Pierre, Proc. SPIE **2776**, 381 (1996).
[14] M. Ohring, *The Materials Science of Thin Films* (Academic, San Diego, 1992), pp. 420–425.
[15] H. Tada, P. Nieva, P. Zavracky, I. N. Miaulis, and P. Y. Wong, Mater. Res. Soc. Symp. Proc. **546** (1999).
[16] S. Hong, T. P. Weihs, J. C. Bravman, and W. D. Nix, Mater. Res. Soc. Symp. Proc. **130**, 93 (1989).
[17] P. H. Townsend and D. M. Barnett, J. Appl. Phys. **62**, 4438 (1987).
[18] X. Ding, W. H. Ko, and J. M. Mansour, Sens. Actuators A **21–23**, 866 (1990).
[19] H. Tada, A. E. Kumpel, R. E. Lathrop, J. B. Slanina, P. Nieva, P. Zavracky, I. N. Miaoulis, and P. Y. Wong (unpublished).
[20] T. P. Weihs, S. Hong, J. C. Bravman, and W. D. Nix, Mater. Res. Soc. Symp. Proc. **130**, 87 (1989).
[21] G. W. McLellan and E. B. Shand, *Glass Engineering Handbook*, 3rd ed. (McGraw–Hill, New York, 1984), 2-14-2-15.